Bioorganic & Medicinal Chemistry xxx (2016) xxx–xxx

Contents lists available at ScienceDirect

Bioorganic & Medicinal Chemistry

journal homepage: www.elsevier.com/locate/bmc

Design and synthesis of phosphoryl-substituted diphenylpyrimidines (Pho-DPPYs) as potent Bruton's tyrosine kinase (BTK) inhibitors: Targeted treatment of B lymphoblastic leukemia cell lines

Yang Ge [a,1], Haijun Yang [a,1], Changyuan Wang [a], Qiang Meng [a], Lei Li [a], Huijun Sun [a], Yuhong Zhen [a], Kexin Liu [a], Yanxia Li [b], Xiaodong Ma [a,*]

[a] College of Pharmacy, Dalian Medical University, Dalian 116044, PR China
[b] Department of Respiratory, The First Affiliated Hospital of Dalian Medical University, Dalian 116011, PR China

ARTICLE INFO

Article history:
Received 16 September 2016
Revised 1 November 2016
Accepted 28 November 2016
Available online xxxx

Keywords:
Leukemia
BTK
DPPY
Phosphoryl
Inhibitor

ABSTRACT

A family of phosphoryl-substituted diphenylpyrimidine derivatives (Pho-DPPYs) were synthesized and biologically evaluated as potent BTK inhibitors in this study. Compound **7b** was found to markedly inhibit BTK activity at concentrations of 0.82 nmol/L, as well as to suppress the proliferations of B-cell leukemia cell lines (Ramos and Raji) expressing high levels of BTK at concentrations of 3.17 μM and 6.69 μM. Moreover, flow cytometry analysis results further indicated that **7b** promoted cell apoptosis to a substantial degree. In a word, compound **7b** is a promising BTK inhibitor for the treatment of B-cell lymphoblastic leukemia.

1. Introduction

Chronic lymphocytic leukemia (CLL), the most common adult leukemia in Western countries, is a neoplastic disease of monoclonal $CD5^+$ B cells which accumulate in the blood, marrow, and secondary lymphoid tissues.[1,2] Bruton's tyrosine kinase (BTK) is an important member of the Tec non-receptor protein kinase family that is always expressed in B cells and myeloid cells. The function of BTK in signaling pathways activated by the engagement of the B cell receptor (BCR) and FCER on mast cells has been well established.[3,4] The unique structure of BTK, which is characterized by a cysteine (Cys481) within the ATP-binding pocket, makes it an attractive therapeutic target.[5,6] Ibrutinib (**1**, Fig. 1) is a first-in-class, irreversible small-molecule inhibitor of BTK that has the ability to covalently bind to Cys481[7–10] and has displayed considerable single-agent activity in patients with relapsed CLL and in previously untreated patients. Disease progression during ibrutinib treatment is uncommon in patients with previously untreated CLL or in patients with low-risk genomic abnormalities.

Until now, several novel preclinical or clinical candidates for the treatment of CLL have been discovered, including acalabrutinib (**2**), (ClinicalTrials.gov identifier: NCT02717611)[11–13], GS-4059 (**3**) (ClinicalTrials.gov identifier: NCT02457559),[14,15] spebrutinib (**4**) (ClinicalTrials.gov identifier: NCT01744626)[16], HM71224 (**5**) (ClinicalTrials.gov identifier: NCT01765478)[17], and PLS-123 (**6**).[18] (Fig. 1). Generally, a pyrimidine core accompanied by an acrylamide group can irreversibly inhibit BTK by using a Michael acceptor to bind to the target Cys481. This is essential for these novel BTK inhibitors to function properly, as depicted in Fig. 1.[8,19–21] The phosphoryl group, which has well-known biological functionality, is often used to improve the aqueous solubility and biological activity of anticancer alkylating agents that require activation *in vivo*.[22–24] In this study, with the primary goal of improving these biological properties, a series of phosphoryl-substituted diphenylpyrimidine derivatives (Pho-DPPYs) were synthesized as potent BTK inhibitors for B-cell lymphoblastic leukemia (Fig. 2). The newly introduced phosphoryl group was observed to form an additional hydrogen bond according to molecular simulations, suggesting that they are effective structural modifiers.

2. Results and discussion

2.1. Chemistry

The synthetic route for the title Pho-DPPYs **7a**–**f** is illustrated in Scheme 1.[25–28] Commercially available chlorine-substituted

* Corresponding author.
E-mail address: xiaodong.ma@139.com (X. Ma).
[1] These authors contributed equally to this work.

http://dx.doi.org/10.1016/j.bmc.2016.11.054
0968-0896/

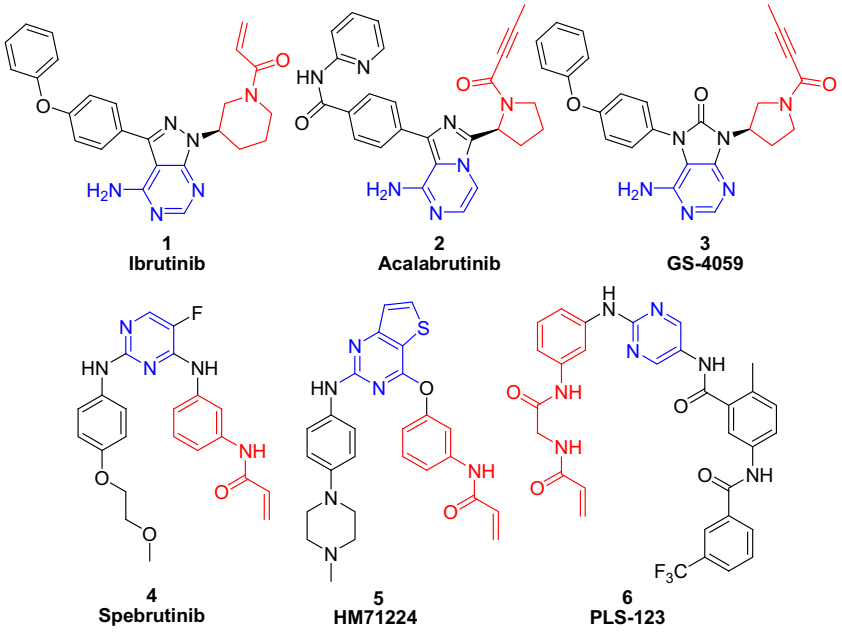

Fig. 1. Structures of the novel BTK inhibitors.

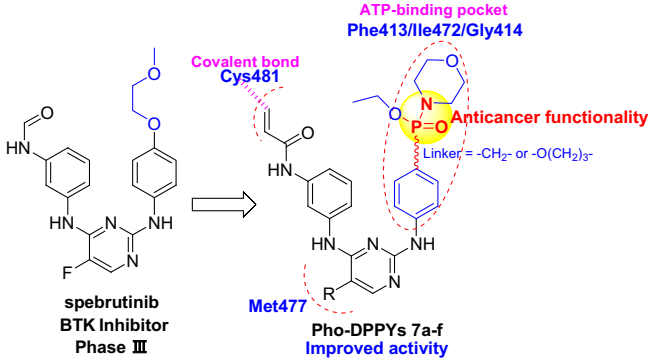

Fig. 2. Designed strategy of Pho-DPPYs as BTK inhibitors.

nitrobenzene **8a**,**b** was reacted with triethylphosphate to provide the diethoxyphosphinyl nitrobenzene **9a**,**b**, which was reduced under Fe-NH_4Cl conditions to form the aniline **10a**,**b**. Compounds **9a**,**b** were treated with thionyl chloride and reacted with morpholine in dichloromethane solvent to produce the amidophosphonates **13a**,**b**. To prepare the 4-chlorine pyrimidines **16a**–**b**, reagent 3-nitroaniline was utilized to create an acylation reaction with acryloyl chlorine under base reagent $NaHCO_3$. Aniline **15**, which was obtained by reducing the nitro group in *N*-acryloyl-4-nitrobenzamide, was regioselectively coupled to the 4-position of 2,4-dichloropyrimidine to create the key intermediate **16a**–**b**. With these intermediates in hand, title molecules **7a**–**f** were synthesized via coupling reaction of **10a**,**b** or **13a**,**b** with **16a**–**b** in the presence of trifluoroacetic acid (TFA) under reflux temperature.

2.2. Biological activity

The title molecules were evaluated in regards to their activity against BTK kinase with an ADP-Glo™ Kinase Assay.[29–31] Their potency for repressing the proliferations of B leukemia cells was observed according to the CCK-8 assay method.[19] Two typical B-cell lymphoblastic leukemia cell lines, Ramos and Raji, which over-expressed BTK enzyme were used for this purpose. In addition, cell cycle and apoptosis rate were analyzed via flow cytometry. For comparison, two novel BTK inhibitors, spebrutinib and ibrutinib, were also tested as reference compounds. The results are provided in Table 1.

According to the kinase-based test results, the Pho-DPPYs effectively inhibited BTK enzyme activity within concentrations of 112.0 nmol/L. Compound **7b** (IC_{50} = 0.82 nM), bearing a 3-morpholin-4-ylpropoxy substituent at the *C*-4 aniline moiety of its pyrimidine core, was the most active inhibitor of BTK. When reducing the linker with a methylene group, the produced molecule **7a** reduced approximately 136-fold anti-BTK activity. The diethoxyphosphinyl-substituted **7c** was also notable, as it likewise displayed strong capacity to inhibit BTK at concentrations of 1.23 nM. Replacing the linker with a long propoxy group was not successful. For instance, inhibitor **7d** reduced about 9-times anti-BTK activity. Installing a fluorine atom at the *C*-5 position of pyrimidine core was less beneficial than the chlorine substituent. The examples **7e** and **7f** with fluorine substituents lost approximately 18 and 29-fold the potency against BTK, respectively.

As shown in Table 1, the Pho-DPPYs were able to inhibit B leukemia cell lines at micromolar concentrations. Inhibitor **7b**, which displayed especially strong potency against BTK kinase, was the most active inhibitor in regards to interfering with the Ramos and Raji cell lines with IC_{50} values of 3.17 μM, and 6.69 μM, respectively. To this effect, compound **7b** exhibited superior biological properties to the references spebrutinib and ibrutinib. Interestingly, molecules **7b**–**d** displayed higher potency in cell viability despite their lower potency against BTK than the references. The introduced phosphinyl substituent was likely the major reason for the improved capability against B leukemia cells.

Inhibitor **7b** was also tested in regards to its effects on the cell cycle and apoptosis of the Ramos cell line via flow cytometry analysis. Again, for comparison, spebrutinib and ibrutinib were also tested. Fig. 3 shows where molecule **7b**, even at a low concentration (5 μM), could induced similar apoptosis rates (45.1%) as spebrutinib (41.5%) and ibrutinib (47.9%) at high concentrations of 10 μM. Cell cycle analysis via flow cytometry indicated that molecule **7b** significantly locked Ramos cells at the G2/M phase. Compared to control group, the percentages of the G2/M phase

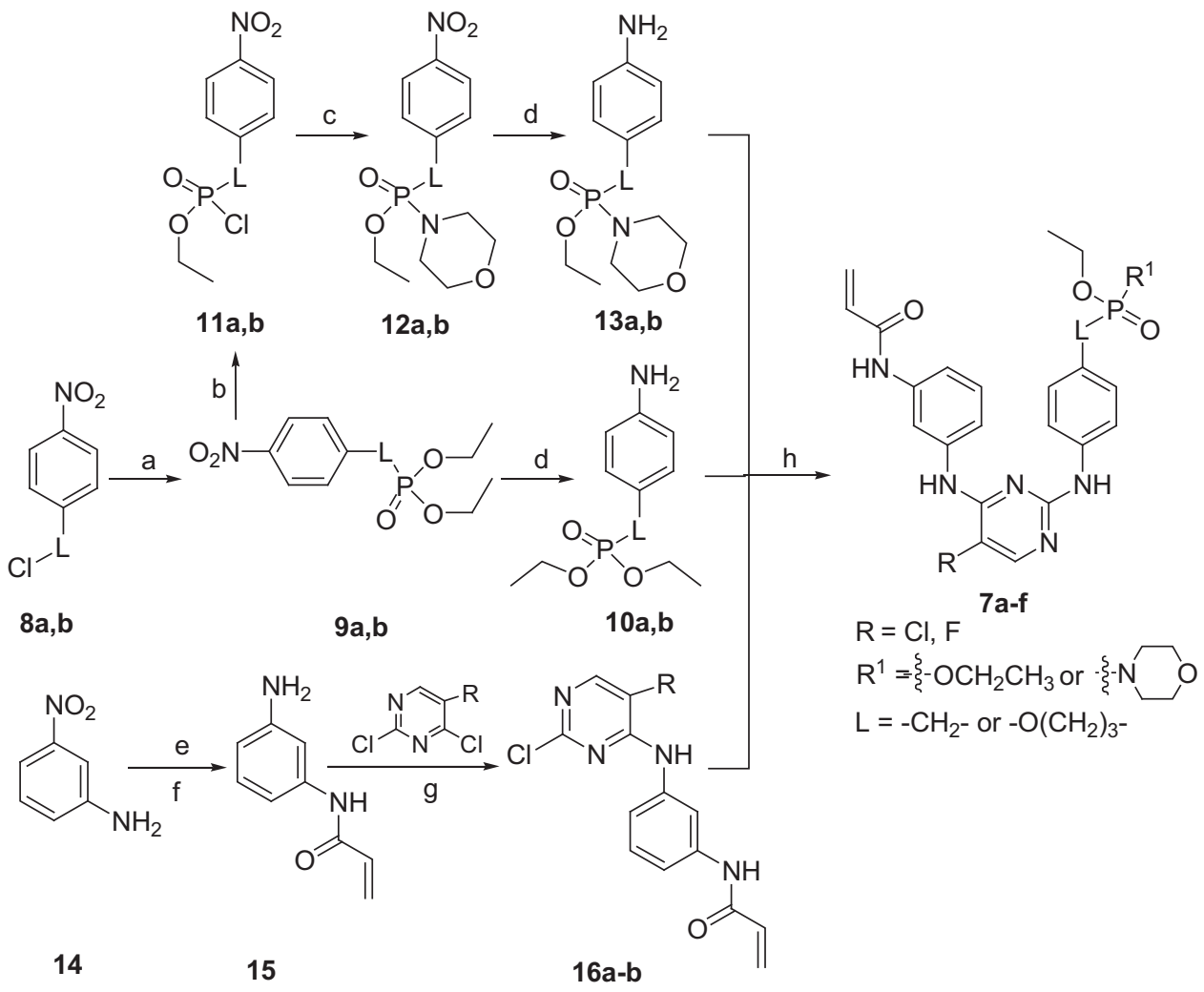

Scheme 1. Synthetic route of the title compounds **7a–f**. Reagents and conditions: (a) $P(OEt)_3$, 5 h, 130 °C, 80–91%; (b) $(COCl)_2$, DMF, 60 °C, 2 h; (c) morpholine, THF, 0 °C, 2 h, 92% (d) Fe-NH_4Cl, MeOH-H_2O, 2 h, 70 °C, 65–78%; (e) acryloyl chloride, $NaHCO_3$, CH_3CN, 0 °C, 0.5 h, 95%; (f) Fe-NH_4Cl, MeOH-H_2O, 2 h, 70 °C, 92%; (g) DIPEA, 1,4-dioxane, 60 °C, 2 h, 91%; (h) trifluoroacetic acid, 2-BuOH, 100 °C, 12 h, 6–20%.

increased from 4.98% to 11.22%, and those of the S phase decreased from 55.1% to 50.8% via treatment with **7b** at concentrations from 1 μM, 5 μM, and 10 μM for 48 h. However, the percentages of the G0/M phase had only minor changes. Apparently, both the new synthesized molecule **7b** and spebrutinib produced similar inhibition results in terms of arresting the cell cycle at the G2/M phase. By contrast, inhibitor ibrutinib arrested the cell cycle at the S phase (Fig. 4).

2.3. Molecular simulations

To elucidate the binding mechanism of the phosphoryl-substituted pyrimidine derivatives, four typical inhibitors, **7b**,**c** (most active), **7f** (moderately active), and **7a** (less potent), were docked individually into the ATP binding pocket of BTK (PDB: 3GEN).[32] The program AutoDock 4.2 (default parameters) was used for this test[33–35]; the docking modes are depicted in Fig. 5.

Apparently, two potent inhibitors, **7b** (Fig. 5a) and **7c** (Fig. 5b), formed several important binding forces with the BTK enzyme, including: 1) the expected covalent bond between the acryl amide group with the amino acid Cys481; 2) hydrogen bond between the oxygen atom of the phosphamide group in compound **7b** with the amino acids Phe413 and Gly414 through a water molecule, or between the amino atom of acryl amide in **7c** with Asp539; 3) hydrophobic contacts generated by the *C*-5 chlorine atom of the pyrimidine core with the amino acid Met477; and 4) π-π contacts produced by the phenyl ring of the *C*-2 aniline moiety with Lys430. Conversely, for the moderately active inhibitor **7f** (Fig. 5c), only the covalent bond and π-π contacts remained at the end of the test. Although the less potent inhibitor **7a** (Fig. 5d) did bind in the ATP-binding pocket, all these important interaction forces were lost during the test process. In a word, these modes were in accordance with their biological activity.

3. Conclusion

A series of phosphoryl-substituted diphenylpyrimidines were synthesized in this exploration with the aim to improve their activity against B-cell leukemia cell lines. Among these novel compounds, **7b** was able to inhibit BTK activity at very low concentrations of 0.82 nmol/L. Moreover, inhibitor **7b** could suppress the proliferations of Ramos cells at concentrations of 3.17 μM and Raji cells at 6.69 μM. Flow cytometry results indicated that **7b** remarkably promoted cell apoptosis, and molecular simulation results showed that **7b** binds tightly with BTK enzyme. Overall, these results suggest that **7b** is a promising BTK inhibitor which

Table 1
Biological activity of the newly synthesized compounds **7a**–**f**.[a]

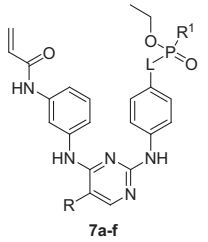

Compound	R	R^1	L	Enzymatic activity (IC_{50}, nM)[b]	Antiproliferative activity (IC_{50}, μM)	
				BTK	Ramos	Raji
7a	Cl		—CH_2—	112.0	27.4	7.71
7b	Cl		—$O(CH_2)_3$—	0.82	3.17	6.69
7c	Cl		—CH_2—	1.23	11.7	13.5
7d	Cl		—$O(CH_2)_3$—	10.6	5.40	6.07
7e	F		—CH_2—	32.1	9.36	34.9
7f	F		—$O(CH_2)_3$—	21.6	11.5	16.4
Spebrutinib				0.72	15.1	25.3
Ibrutinib				0.34	5.14	19.5

[a] Data represent the mean of at least three separate experiments.
[b] The IC_{50} values are the concentrations in micromolar needed to inhibit cell growth by 50% as, as calculated using GraphPad Prim version 5.0.

may merit further development as a B lymphoblastic leukemia treatment.

4. Experiential section

4.1. General methods and chemistry

All solvents and reagents were obtained from commercial supplies and were used as received. High resolution ESI-MS were performed on an AB Sciex TripleTOF® 4600 LC/MS/MS system. ^{1}H NMR and ^{13}C NMR spectra on a Brucker AV 400 MHz spectrometer were recorded in [*d*] DMSO. Coupling constants (*J*) are expressed in hertz (Hz). Chemical shifts (δ) of NMR are reported in parts per million (ppm) units relative to internal control (TMS). ^{1}H NMR spectra are reported in the following order: multiplicity, approximate coupling constant (*J* value) in hertz, and number of protons; signals are characterized as s (singlet), d (doublet), dd (doublet of doublets), t (triplet), dt (doublet of triplets), q (quartet), m (multiplet), and br s (broad signal). All reactions were monitored by TLC, using silica gel plates with fluorescence F254 (TLC Silica gel 60 F254, Merck) and UV light visualization. Flash chromatography separations were obtained on Silica Gel (300–400 mesh) using dichloromethane/methanol as eluents.

4.2. General procedure for the synthesis of ***7a***–***f***[25–28]

Phosphoryl-substituted anilines **10a**,**b** and **13a**,**b** were prepared according to the literatures.[23,24] While the intermediates *N*-(3-((2-chloro-5-substitutedpyrimidin-4-yl)oxy)phenyl)acrylamides **16a**,**b** were synthesized using the procedures reported in Refs. 21,22. All these intermediates were directly used without any purification and structural characterization. With these intermediates in hand, the newly obtained compounds were synthesized as described below.

A flask was charged with 2-chlorine-substituted pyrimidine **16a**,**b** and aniline **10a**,**b** (0.70 mmol), or **13a**,**b** (0.70 mmol), TFA (0.08 mL, 1.05 mmol), and 2-BuOH (10 mL).The slurry was heated to 100 °C for 10 h. The reaction mixture was allowed to cool to room temperature and was neutralized with a saturated aqueous sodium bicarbonate solution. The aqueous mixture was then extracted with CH_2Cl_2 (20 mL) three times. The crude product was purified using flash chromatography with dichloromethane/methanol (v/v, 30:1) as eluents.

4.2.1. *N*-(3-((5-Chloro-2-((4-(((1-morpholino)ethoxyphosphinyl)methy))amino)phenylamino-4-pyrimidinyl)amino)phenyl)acrylamide (***7a***)

Off-white solid (172 mg, 15.6%); ^{1}H NMR (400 MHz, DMSO-d_6): δ 10.18 (s, 1H), 9.29 (s, 1H), 8.95 (s, 1H), 8.14 (s, 1H), 7.86 (s, 1H), 7.63–7.41 (m, 3H), 7.40–7.25 (m, 2H), 7.03 (d, *J* = 7.0 Hz, 2H), 6.46 (dd, *J* = 16.9 10.1 Hz, 1H), 6.26 (d, *J* = 16.8 Hz, 1H), 5.75 (d, *J* = 10.0 Hz, 1H), 4.00–3.76 (m, 2H), 3.40 (d, *J* = 3.1 Hz, 4H), 2.93 (dd, *J* = 55.4, 27.9 Hz, 6H), 1.20 (t, *J* = 7.0 Hz, 3H); ^{13}C NMR (400 MHz, DMSO-d_6): δ 163.1 157.6, 156.2, 154.8, 139.1, 138.8 (d, *J* = 38.8 Hz), 131.9, 129.7 (d, *J* = 25.2 Hz), 128.5, 126.9, 125.0, 124.9, 119.4, 118.7 (2C), 115.5, 115.2, 103.8, 66.4 (d, *J* = 18.8 Hz,

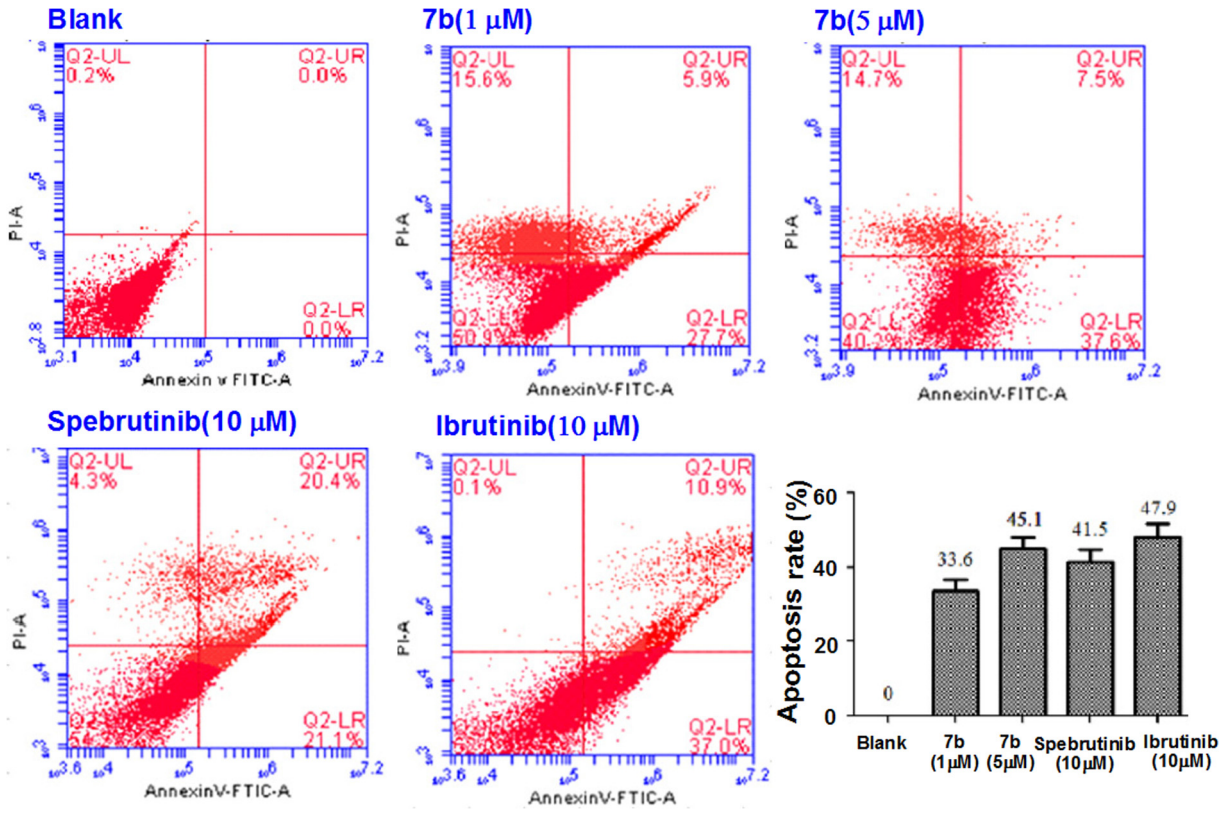

Fig. 3. Compound **7b** induced Ramos cell apoptosis *in vitro*. The cells were incubated with the indicated concentrations of **7b** for 48 h, and the cells were stained with annexin V/FTIC, followed by flow cytometry analysis. One representative experiment is shown. $p < 0.05$.

2C), 59.1 (d, J = 27.6 Hz), 43.7 (2C), 32.6, 31.3, 16.3 (d, J = 24.8 Hz); HRMS (ESI) m/z calcd for $C_{26}H_{30}ClN_6O_4P$ $[M+H]^+$ 557.1833, found 557.1790.

*4.2.2. N-(3-((5-Chloro-2-((4-(((1-morpholino)ethoxyphosphinyl) propoxyl))amino)phenylamino-4-pyrimidinyl)amino)phenyl) acrylamide (**7b**)*

Off-white solid (50 mg, 6.8%); ^{1}H NMR (400 MHz, DMSO-d_6): δ 10.21 (s, 1H), 9.16 (s, 1H), 8.89 (s, 1H), 8.10 (s, 1H), 7.89 (s, 1H), 7.52 (dd, J = 34.2, 8.8 Hz, 3H), 7.30 (d, J = 4.9 Hz, 2H), 6.69 (d, J = 8.3 Hz, 2H), 6.46 (dd, J = 16.9, 10.1 Hz, 1H), 6.25 (d, J = 16.8 Hz, 1H), 5.76 (d, J = 10.0 Hz, 1H), 4.10–3.76 (m, 4H), 3.56 (d, J = 35.6 Hz, 4H), 2.94 (t, J = 38.4 Hz, 4H), 2.05–1.68 (m, 4H), 1.21 (t, J = 7.0 Hz, 3H); ^{13}C NMR (400 MHz, DMSO-d_6): δ 163.1, 157.8, 156.1, 154.8, 153.1, 139.0, 138.9(d, J = 60.8 Hz), 133.6, 131.9, 128.6, 126.9, 120.5 (2C), 119.1, 115.4 (d, J = 57.2 Hz), 114.1 (2C), 103.2, 67.3 (d, J = 67.6 Hz), 66.6 (d, J = 19.6 Hz, 2C), 58.8 (d, J = 26.4 Hz), 43.5 (2C), 22.5 (d, J = 18.0 Hz), 21.9, 20.5, 16.3 (d, J = 24.4 Hz); HRMS (ESI) m/z calcd for $C_{28}H_{34}ClN_6O_5P$ $[M+H]^+$ 601.2090, found 601.2044.

*4.2.3. N-(3-((5-Chloro-2-((4-((diethoxyphosphoryl)methy))amino) phenylamino-4-pyrimidinyl)amino)phenyl)acrylamide (**7c**)*

Off-white solid (190 mg, 18.9%); ^{1}H NMR (400 MHz, DMSO-d_6): δ 10.19 (s, 1H), 9.31 (s, 1H), 8.95 (s, 1H), 8.14 (s, 1H), 7.86 (s, 1H), 7.61–7.41 (m, 3H), 7.40–7.22 (m, 2H), 7.01 (d, J = 6.7 Hz, 2H), 6.46 (dd, J = 17.0, 10.1 Hz, 1H), 6.26 (dd, J = 17.0, 1.8 Hz, 1H), 5.75 (dd, J = 10.2, 1.8 Hz, 1H), 3.99–3.81 (m, 4H), 3.06 (d, J = 21.1 Hz, 2H), 1.15 (t, J = 7.0 Hz, 6H); ^{13}C NMR (400 MHz, DMSO-d_6): δ 163.4, 157.9, 156.4, 155.0, 139.4, 139.1 (d, J = 20.8 Hz), 132.1, 129.8 (d, J = 26.0 Hz), 128.7, 127.1, 124.7, 124.6, 119.6, 118.9 (2C), 115.7, 115.4, 104.0, 61.5 (d, J = 25.6 Hz, 2C), 32.5, 31.1, 16.5 (d, J = 22.4 Hz, 2C); HRMS (ESI) m/z calcd for $C_{24}H_{27}ClN_5O_4P$ $[M+H]^+$ 516.1562, found 516.1488.

*4.2.4. N-(3-((5-Chloro-2-((4-((diethoxyphosphoryl)propoxyl))amino) phenylamino-4-pyrimidinyl)amino)phenyl)acrylamide (**7d**)*

Off-white solid (123 mg, 11.0%); ^{1}H NMR (400 MHz, DMSO-d_6): δ 10.18 (s, 1H), 9.15 (s, 1H), 8.90 (s, 1H), 8.10 (s, 1H), 7.88 (s, 1H), 7.57–7.40 (m, 3H), 7.31 (d, J = 5.2 Hz, 2H), 6.69 (d, J = 8.8 Hz, 2H), 6.46 (dd, J = 17.0, 10.1 Hz, 1H), 6.26 (dd, J = 17.0, 2.0 Hz, 1H), 5.76 (dd, J = 10.2, 2.0 Hz, 1H), 4.05–3.88 (m, 6H), 1.92–1.79 (m, 4H), 1.23 (t, J = 7.0 Hz, 6H); ^{13}C NMR (400 MHz, DMSO-d_6): δ 163.3, 158.0, 156.3, 155.0, 153.3, 139.2, 139.1, 133.9, 132.1, 128.8, 127.1, 120.7 (2C), 119.4, 115.6 (d, J = 57.2 Hz), 114.3 (2C), 103.4, 67.3 (d, J = 68.0 Hz), 61.2 (d, J = 24.8 Hz, 2C), 22.5 (d, J = 18.0 Hz), 22.1, 20.7, 16.5 (d, J = 22.8 Hz, 2C); HRMS (ESI) m/z calcd for $C_{26}H_{31}ClN_5O_5P$ $[M+H]^+$ 560.1824, found 560.1731.

*4.2.5. N-(3-((5-Fluorine-2-((4-((diethoxyphosphoryl)methy))amino) phenylamino-4-pyrimidinyl)amino)phenyl)acrylamide (**7e**)*

Off-white solid (136 mg, 12.7%); ^{1}H NMR (400 MHz, DMSO-d_6): δ 10.16 (s, 1H), 9.44 (s, 1H), 9.17 (s, 1H), 8.11 (d, J = 2.7 Hz, 1H), 7.93 (s, 1H), 7.57 (dd, J = 16.8, 7.9 Hz, 3H), 7.44 (d, J = 7.5 Hz, 1H), 7.29 (t, J = 7.9 Hz, 1H), 7.06 (d, J = 6.8 Hz, 2H), 6.47 (dd, J = 16.8, 10.2 Hz, 1H), 6.26 (d, J = 16.8 Hz, 1H), 5.76 (d, J = 10.0 Hz, 1H), 4.09–3.77 (m, 4H), 3.08 (d, J = 21.0 Hz, 2H), 1.16 (t, J = 6.8 Hz, 6H); ^{13}C NMR (400 MHz, DMSO-d_6): δ 163.1, 155.5 (d, J = 10.4 Hz), 149.8 (d, J = 43.6 Hz), 141.8, 140.8 (d, J = 76.8 Hz), 139.4 (d, J = 12.8 Hz), 139.1 (d, J = 28.0 Hz), 132.0, 129.6 (d, J = 25.2 Hz), 128.6, 126.9, 124.2, 124.1, 118.4 (2C), 117.5, 114.8, 113.3, 61.3 (d, J = 25.6 Hz, 2C), 32.3, 30.9, 16.3 (d, J = 22.4 Hz, 2C); HRMS (ESI) m/z calcd for $C_{24}H_{27}FN_5O_4P$ $[M+H]^+$ 500.1857, found 500.1786.

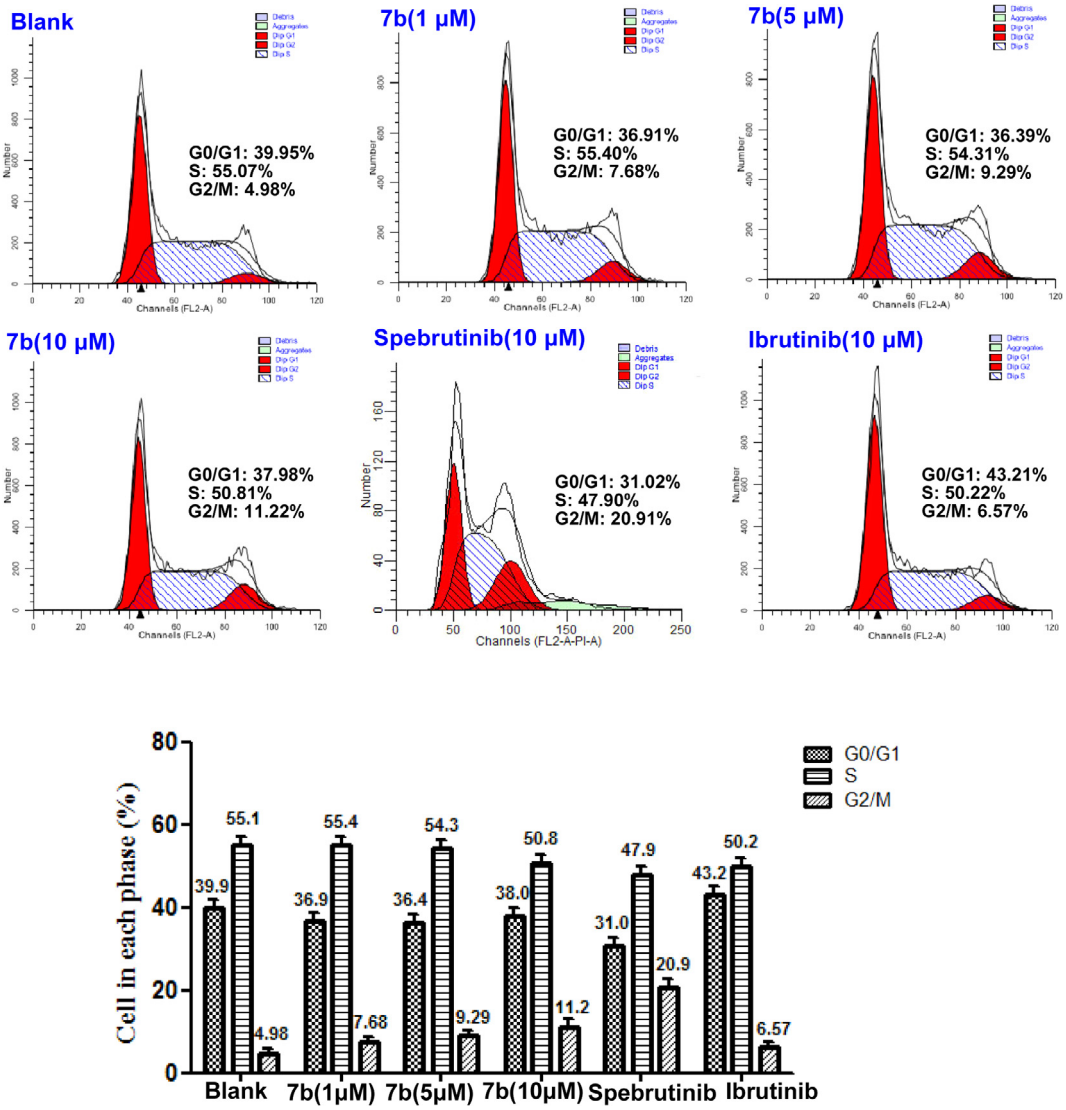

Fig. 4. Effects of spebrutinib, ibrutinib and **7b** on Ramos cell cycle arrest detected by flow cytometry assay. Results are representative of three separate experiments, dates are expressed as the mean ± standard deviation, $p < 0.05$.

*4.2.6. N-(3-((5-Fluorine-2-((4-((diethoxyphosphoryl)propoxyl)) amino)phenylamino-4-pyrimidinyl)amino)phenyl)acrylamide (**7f**)*

Off-white solid (52 mg, 7.0%); ^{1}H NMR (400 MHz, DMSO-d_6): δ 10.13 (s, 1H), 9.38 (s, 1H), 8.98 (s, 1H), 8.06 (d, J = 3.7 Hz, 1H), 7.93 (s, 1H), 7.51 (dd, J = 13.1, 9.2 Hz, 3H), 7.42 (d, J = 8.1 Hz, 1H), 7.28 (t, J = 8.1 Hz, 1H), 6.75 (d, J = 9.0 Hz, 2H), 6.46 (dd, J = 16.9, 10.1 Hz, 1H), 6.26 (dd, J = 17.0, 1.9 Hz, 1H), 5.76 (dd, J = 10.2, 1.8 Hz, 1H), 4.22–3.67 (m, 6H), 1.92–1.79 (m, 4H), 1.22 (t, J = 7.0 Hz, 6H); ^{13}C NMR (400 MHz, DMSO-d_6): δ 163.3, 155.9 (d, J = 10.4 Hz), 153.2, 150.0 (d, J = 42.8 Hz), 141.8, 141.1 (d, J = 74.8 Hz), 139.3 (d, J = 28.0 Hz), 134.4, 132.2, 128.9, 127.1, 120.5 (2C), 117.6, 115.0, 114.4 (2C), 113.6, 67.4 (d, J = 68.4 Hz), 61.2 (d, J = 25.2 Hz, 2C), 22.5 (d, J = 18.4 Hz), 22.1, 20.7, 16.5 (d, J = 22.8 Hz, 2C); HRMS (ESI) m/z calcd for $C_{26}H_{31}FN_5O_5P$ $[M+H]^+$ 544.2120, found 544.2019.

4.3. In vitro kinase enzymatic assay

The BTK kinase enzyme system (Catalog. V9071) was purchased from Promega Corporation (USA). Concentrations consisting of suitable levels from 0.1 to 100 nM were used for all of the tested compounds. The experiments were performed according to the instructions of the manufacturer. The more detailed and complete protocols, see the ADP-Glo™ kinase Assay Technical Manual available at: http://cn.promega.com/resources/protocols/product-information-sheets/n/btk-kinase-enzyme-system-protocol/. The test was performed in a 384-well plate, and includes the major steps below: (1) perform a 5 μL kinase reaction using 1× kinase buffer (e.g., 1× reaction buffer A), (2) incubate at room temperature for 60 min, (3) add 5 μL of ADP-Glo™ Reagent to stop the kinase reaction and deplete the unconsumed ATP, leaving only ADP and a very low background of ATP, (4) incubate at room temperature for 40 min, (5) add 10 μL of Kinase Detection, (6) reagent to convert ADP to ATP and introduce luciferase and luciferin to detect ATP, (7) incubate at room temperature for 30 min, (8) plate was measured on TriStar® LB942 Multimode Microplate Reader (BERTHOLD) to detect the luminescence (Integration time 0.5–1 s). Curve fitting and data presentations were performed using GraphPad Prism version 5.0.[29–31]

4.4. Cellular activity assay

All the cell viability assays were performed according to the CCK-8 method. The cells were seeded in 96-well plates at a density

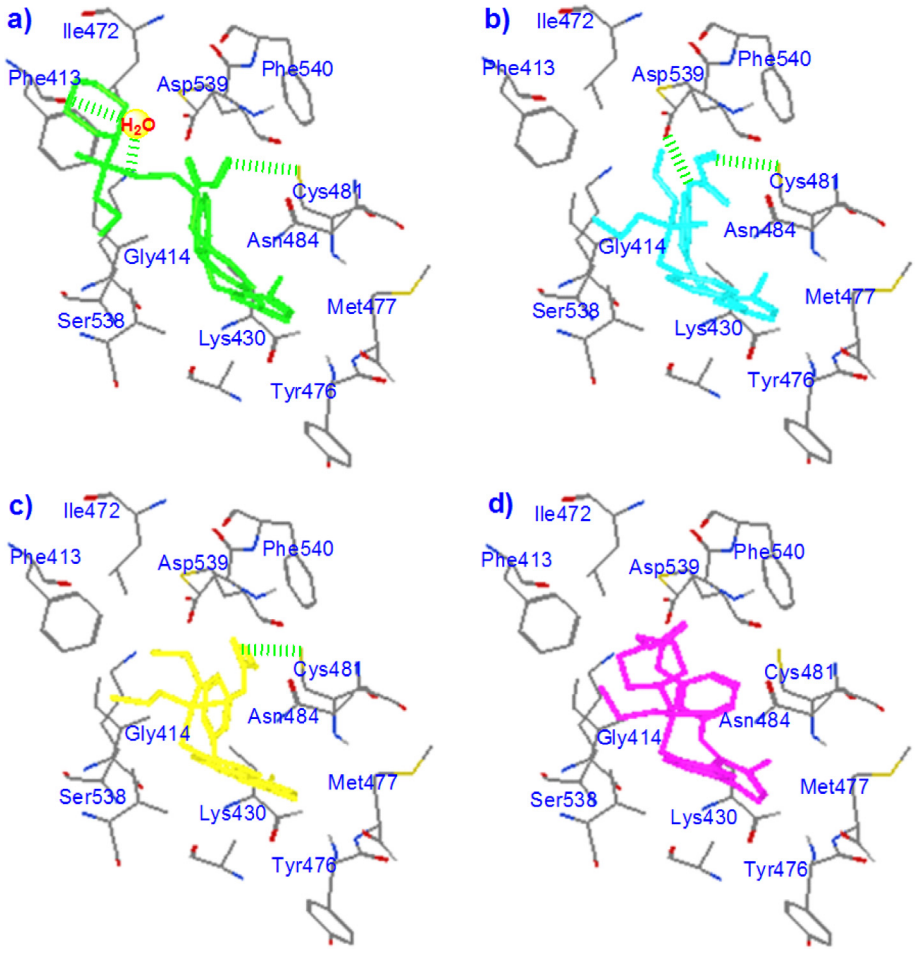

Fig. 5. a) Putative binding mode of inhibitor **7b** within BTK (PDB code: 3GEN). b) Putative binding mode of inhibitor **7c** within BTK (PDB code: 3GEN). c) Putative binding mode of inhibitor **7f** within BTK (PDB code: 3GEN). d) Putative binding mode of inhibitor **7a** within BTK (PDB code: 3GEN).

of 2000–3000 cells/well and were maintained at 37 °C in a 5% CO_2 incubator in RPMI1640 containing 10% fetal bovine serum (FBS, Gibco) for one day. Cells were exposed to treatment for 48 h, and the number of cells used per experiment for each cell lines was adjusted to obtain an absorbance of 0.5–1.2 at 450 nm with a microplate reader (Thermo, USA). Compounds were tested at appropriate concentrations (1.25–40 μM), with each concentration duplicated five times. The IC_{50} values were calculated using GraphPad Prim version 5.0.

4.5. Cell apoptosis assay

The Ramo cells (1–5 × 10^5 cells/well) incubated in 6-well plates were treated with solvent control (DMSO), spebrutinib, ibrutinib, or compound **7b** in medium containing 5% FBS for 48 h. Then, collected and fixed with 70% ethanol at 4 °C overnight. After being fixed with 75% ethanol at 4 °C for 24 h, the cells were stained with Annexin V-FITC (5 μL)/propidium iodide (5 μL), and analyzed by flow cytometry assay (Becton-Dickinson, USA). For cell cycle analysis, Ramos cells at a density of approximately 2 × 10^5 cells/well were incubated in 6-well plates, treated with different concentrations of inhibitors for 48 h, collected and fixed with 70% ethanol at 4 °C overnight. After fixation, the cells were washed with PBS and stained with propidium iodide (PI) for 10 min under subdued light. Stained cells were analyzed flow cytometry assay (Becton-Dickinson, NJ, USA), and the results were performed using FCS Express flow cytometry analysis software (ModFit LT 3.1).

4.6. Molecular docking study

The crystal structure (PDB: 3GEN) of the kinase domain of BTK bound to a pyrrolopyrimidine-containing compound.[32] The enzyme preparation and the hydrogen atoms adding was performed in the prepared process. The whole BTK enzyme was defined as a receptor and the site sphere was selected on the basis of the binding location of pyrrolopyrimidine inhibitor. By moving the inhibitor and the irrelevant water, molecules **7a–c**, **7f** were placed, respectively. The binding interaction energy was calculated to include van der Waals, electrostatic, and torsional energy terms defined in the tripos force field. Ten docking poses were generated and clustered, and compounds with predicted binding affinities better than 7.0 kcal/mol in each of the three docking runs were selected for further analysis and visual inspection. The structure optimization was performed using a genetic algorithm, and only the best-scoring ligand protein complexes were kept for analyses.[33–35] The WWW site also includes many resources for use of AutoDock, including detailed Tutorials that guide users through basic AutoDock usage, docking with flexible rings, and virtual screening with AutoDock. Tutorials may be found at: http://autodock.scripps.edu/faqs-help/tutorial.

Acknowledgments

We are grateful to the National Natural Science Foundation of China (No. 81402788), the PhD Start-up Fund of Natural Science

Foundation of Liaoning Province, China (No. 20141115), and the Cultivation Project of Youth Techstars, Dalian (No. 2016RQ043) for the financial support of this research.

A. Supplementary data

Supplementary data associated with this article can be found, in the online version, at http://dx.doi.org/10.1016/j.bmc.2016.11.054.

References

1. Hallek M. *Blood*. 2013;122:3723.
2. Cramer P, Hallek M. *Nat Rev Clin Oncol*. 2011;8:38.
3. Schmidt U, Boucheron N, Unger B, Ellmeier W. *Int Arch Allergy Immunol*. 2004;134:65.
4. Berg LJ, Finkelstein LD, Lucas JA, Schwartzberg PL. *Annu Rev Immunol*. 2005;23:549.
5. Cohen MS, Zhang C, Shokat KM, Taunton J. *Science*. 2005;308:1318.
6. Leproult E, Barluenga S, Moras D, Wurtz JM, Winssinger N. *J Med Chem*. 2011;54:1347.
7. Davis RE, Ngo VN, Lenz G, et al. *Nature*. 2010;463:88.
8. Pan Z, Scheerens H, Li SJ, et al. *ChemMedChem*. 2007;2:58.
9. Honigberg LA, Smith AM, Sirisawad M, et al. *Proc Natl Acad Sci USA*. 2010;107:13075.
10. de Rooij MF, Kuil A, Geest CR, et al. *Blood*. 2012;119:2590.
11. Byrd JC, Harrington B, O'Brien S, et al. *N Engl J Med*. 2016;374:323.
12. Harrington BK, Gardner HL, Izumi R, et al. *PLoS One*. 2016;11:e0159607.
13. Wu J, Zhang M, Liu DJ. *Hematol Oncol*. 2016;9:1.
14. Walter HS, Rule SA, Dyer MJ, et al. *Blood*. 2016;127:411.
15. Jones R, Axelrod MJ, Tumas D, Quéva C, Paolo JD. *Blood*. 2016;126:1749.
16. Evans E, Ponader S, Karp R, et al. *Clin Lymphoma Myeloma Leuk*. 2011;11:S173.
17. Park JK, Byun JY, Park JA, et al. *Arthritis Res Ther*. 2016;18:91.
18. Li X, Zuo Y, Tang G, et al. *J Med Chem*. 2014;57:5112.
19. Wu H, Wang W, Liu F, et al. *ACS Chem Biol*. 2014;9:1086.
20. Santos-Garcia L, Assisa LC, Silva DR, Ramalho TC, da Cunha EF. *J Biomol Struct Dyn*. 2016;34:1421.
21. Xu A, Zhang Y, Ran T, et al. *SAR QSAR Environ Res*. 2015;26:279.
22. Alberts DS, Hallum III AV, Stratton-Custis M, et al. *Clin Cancer Res*. 2001;7:1246.
23. Huttunen KM, Rautio J. *Curr Top Med Chem*. 2011;11:2265.
24. Jain M, Fan J, Baturay NZ, Kwon CH. *J Med Chem*. 2004;47:3843.
25. Zhou W, Ercan D, Chen L, et al. *Nature*. 2009;462:1070.
26. Han C, Huang Z, Zheng C, et al. *J Med Chem*. 2013;56:4738.
27. Martinez Farias MA, Kincaid VA, Annamalai VR, Kiessling LL. *J Am Chem Soc*. 2014;136:8492.
28. Yoshino K, Goto K, Yoshiizumi K, Morita T, Tsukamoto G. *J Med Chem*. 1990;33:2192.
29. Cizdziel JV, Tolbert C, Brown G. *Spectrochim Acta B*. 2010;65:176.
30. Somberg R, Pferdehirt B, Kupcho AK. *Cell Notes*. 2003;5:5.
31. Zegzouti H, Zdanovskaia M, Hsiao K, Goueli SA. *Assay Drug Dev Technol*. 2009;7:560.
32. Marcotte DJ, Liu YT, Arduini RM, et al. *Protein Sci*. 2010;19:429.
33. Wildman SA, Zheng X, Sept D, Auletta JT, Rosenberry TL, Marshall GR. *Chem Biol Drug Des*. 2011;78:495.
34. Ragunathan A, Ravi L. *Der Pharma Lett*. 2015;7:68.
35. Goodsell DS, Morris GM, Olson AJ. *J Mol Recognit*. 1996;9:1.